SAE INTERNATIONAL

ARTICLE INFO
Article ID: 02-14-04-0031

doi:10.4271/02-14-04-0031

Design and Optimization of Forced-Air Cooling System for Commercial Vehicle Brake System

Dengzhi Peng,[1] Gangfeng Tan,[1] Jingning Tang,[2] and Xuexun Guo[1]

[1]Wuhan University of Technology, China
[2]Suizhou Institute of Product Quality Supervision and Inspection, China

Abstract

To maintain the vehicle speed in a proper range, the commercial vehicle needs to brake frequently on a downhill path. The drum brake system of the medium- and heavy-duty commercial vehicles often faces the danger of brake fade, which reduces brake efficiency or even causes braking failure. They are critical potential risks on the road.

The kinetic energy is transferred into thermal energy during the braking process. The temperature rises dramatically during the braking process due to the massive thermal energy caused by the huge mass of the commercial vehicle. The brake efficiency and the life of the brake drum will decrease with the rising temperature. A malfunction of the brake system may occur if the drum brake is overheated. To improve the cooling efficiency of the drum brake, a forced-air cooling system driven by the air compressor in the diesel is designed for the drum brake system after the analysis of its thermal model. A computational fluid dynamics (CFD) model is established and modified after comparison with the test result. Based on this modified model, the parameters of this system are optimized through adaptive particle swarm optimization (APSO).

This optimized forced-air cooling system decreases the maximum temperature of the brake system from 291.9°C to 200°C under the most critical work condition. It allows the commercial vehicle to operate in a safer situation with a lighter weight compared to the current water cooling system.

History

Received: 11 Jun 2020
Revised: 23 Aug 2020
Accepted: 08 Feb 2021
e-Available: 12 Mar 2021

Keywords

Commercial vehicle, Forced-air cooling system, CFD, APSO

Citation

Peng, D., Tan, G., Tang, J., and Guo, X., "Design and Optimization of Forced-Air Cooling System for Commercial Vehicle Brake System," *SAE Int. J. Commer. Veh.* 15(1):15-25, 2022, doi:10.4271/02-14-04-0031.

ISSN: 1946-391X
e-ISSN: 1946-3928

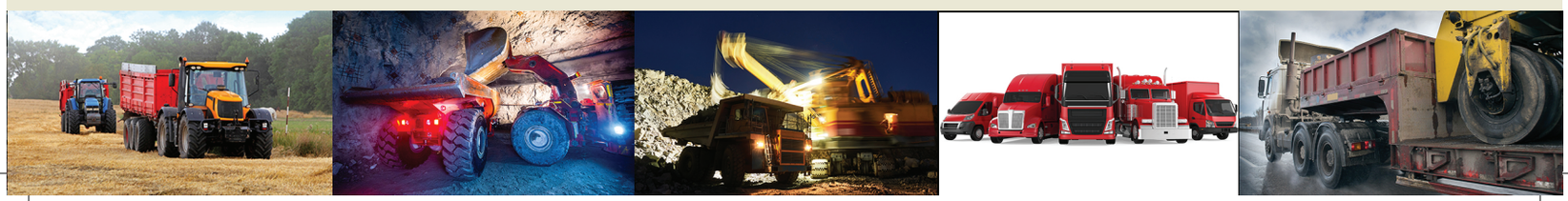

Introduction

The braking performance of a vehicle has a crucial impact on vehicle safety. To make sure a vehicle can stop as the driver intended, the brake system is required to transform large amounts of kinetic energy into heat over very short periods, especially for medium- and heavy-duty commercial vehicles. During the braking process, all parts of the foundation brake need to resist the high temperature, steep temperature gradients, and substantial thermal stresses. Overheat of the brake system causes noise, brake fade, or even malfunction [1]. Despite the mechanical loading, friction force, and rotational stresses, the most critical design parameters of the system relate to thermal loads. Therefore, a lower temperature rise of the brake system can lightweight the whole system and improve vehicle safety.

A lot of researches have been done to analyze the thermal load of the brake system. Yang et al. provided an inverse algorithm based on the conjugate gradient method, and the discrepancy principle is applied to estimate the unknown space- and time-dependent heat flux of the disc in a disc brake system from the knowledge of temperature measurements taken within the disc [2]. Singh et al. and Mule et al. investigated the thermal failure of the drum and disc brake system by finite element analysis (FEA), respectively [3, 4]. The predicted temperature is validated by the experiments in their researches. The computational fluid dynamics (CFD) model is also widely used in the analysis of the brake system; earlier researchers ignore the influence of tires [5, 6]. The error between the simulation and test result ranges from 5% to 20%. The tire is taken into consideration in other researches. Bhambare et al. established a CFD model to analyze the disc brake system [7]. Travaglia et al. analyzed the unsteady heat dissipation process of a truck by a CFD model; the results are validated by an experimental test [8]. Shah and Patidar compared the performance of the disc and drum brake in a commercial vehicle [9]. Mahammad et al. developed a CFD model to predict the temperature of the disc brake and a FEM model to analyze the thermal coning of it [10]. The error between the simulated temperature and test result is narrowed to 2.7%. According to the current research, FEM and CFD are effective methods to analyze the thermal problems of the brake system. Normally, the FEM is used to analyze the generating process of the thermal energy, it focuses on the structure of the brake system, and the CFD is used to analyze the dissipation process of thermal energy.

To lower the temperature of the brake system component, researchers have provided some methods based on simulation. Some of them focused on increasing the airflow around the brake system, while others concentrate on improving the surface contact to the air. Raja et al. designed a duct to supply more air to the rotor surface of the disc-based brake system in a passenger vehicle using the CFD model [11]. Ocampo et al. proposed the aerodynamic impact and cooling performance of the brake system, more airflow to the brake system may end up with a bigger wind drag coefficient [12]. Kim et al. optimized the duct of the brake system by the response surface method (RSM), the extra air drag resistance caused by the duct is decreased [13]. This solution is based on a passenger car; for a commercial vehicle, the more critical temperature rise occurs at the rear axle. It is difficult to set up a duct near the rear axle. Sunday et al. extended the drum surface along its circumference to improve the heat dissipation ability of the drum [14]. This solution needs to redesign the outer surface of the drum and decrease the gap between the drum and rim.

Since there are multiple objectives and factors in the designing of the brake system, multi-objective optimizations, such as NSGA-II (Non-dominated Sorting Genetic Algorithm-II) [15] and CC-MOPSO (Co-Constraint Multi-Objective Particle Swarm Optimization) [16], are used in this area.

Most of the medium- or heavy-duty vehicles are equipped with an extra water tank, using a water-spraying cooling system to maintain the temperature of the brake drum in a proper range. This system needs the driver to keep an eye on the water tank before and within the article, and the cooling water also lowers the weight of the cargo. In addition, spraying water may harm the safety of other vehicles, especially passenger cars [17]. To keep the braking drum temperature of a commercial vehicle in a safe range, a forced-air cooling system is provided based on the mathematic analysis and optimized by the CFD model and APSO. By increasing the airflow around the brake drum through some nozzles near the gap between the rim and drum, the temperature of the drum is decreased. This system is powered by the compressor on the engine and can lower the brake drum temperature in the most critical condition.

Mathematical Model

For a moving vehicle with a gross mass of M, when the speed decelerates from v_1 to v_2, the decreased kinetic energy ΔQ_{ke} during the braking process can be calculated by the following equation:

$$\Delta Q_{ke} = 1/2M\left(v_1^2 - v_2^2\right) \quad \text{Eq. (1)}$$

The decreased kinetic energy is transferred into eight kinds of ways. The "braking energy," ΔQ_b, that is absorbed by the braking system, the wind resistance (ΔQ_{wr}), tire rolling resistance (ΔQ_{rr}), transmission losses (ΔQ_{tr}), engine braking (ΔQ_{eng}), a retarder (ΔQ_{ret}), regenerative braking (ΔQ_{reg}), and potential slope energy (ΔQ_g). The braking energy can be estimated by the following equation [18]:

$$\Delta Q_b = \Delta Q_{ke} - \Delta Q_{wr} - \Delta Q_{rr} - \Delta Q_{tr} - \Delta Q_{eng} - \Delta Q_{ret} - \Delta Q_{reg} \pm \Delta Q_g \quad \text{Eq. (2)}$$

To predict the thermal performance of each brake, the proportion of the whole vehicle braking energy bust be divided. This can be done by using the vehicle's braking distribution

coefficient, which defines the braking force generated by each brake to achieve the desired vehicle deceleration. Divide the equivalent "braking energy" to each wheel by the braking distribution coefficient X_i.

$$\Delta Q_{bi} = X_i \Delta Q_b \qquad \text{Eq. (3)}$$

Taking the structural characteristics into consideration, the method to estimate the energy distributed to the drum, Q_d, and shoe, Q_s, is provided.

$$Q_d = \Delta Q_{bi}\left[\frac{A_d\sqrt{k_d\rho_d c_{pd}}}{A_d\sqrt{k_d\rho_d c_{pd}} + A_s\sqrt{k_s\rho_{sd}c_{ps}}}\right] \qquad \text{Eq. (4)}$$

$$Q_s = \Delta Q_{bi}\left[\frac{A_s\sqrt{k_s\rho_s c_{ps}}}{A_d\sqrt{k_d\rho_d c_{pd}} + A_s\sqrt{k_s\rho_s c_{ps}}}\right] \qquad \text{Eq. (5)}$$

In Equations 4 and 5, A_d and A_s are the friction surface area of the drum and shoe, k is the thermal conductivity, ρ is the mass density, and c_p is the specific heat. According to these equations and parameters of regular commercial vehicles, over 96% of energy is distributed to the drum.

The temperature rise (ΔT) of each brake can be estimated from the energy entering the brake component, the component mass (m) that is expected to be heated, and its specific heat (C_p).

$$\Delta T = Q_d / \left(mC_p\right) \qquad \text{Eq. (6)}$$

Heat dissipation is essential in the brake system, it is made up of three modes of transfer: conduction, convection, and radiation. Among them, conduction is the prime mode of heat dissipation. The air around the brakes is vital to heat dissipation and cooling. Newcomb and Spurr explained how the brake cooling process could be analyzed using Newton's law of cooling in Equation 7 [19].

$$\left(T_t - T_0\right) = \left(T_{t1} - T_0\right)e^{-bt} \qquad \text{Eq. (7)}$$

where T_0 is the ambient temperature, T_t is the temperature of the drum at time t, T_{t1} is the temperature of the drum at the start of cooling, t means time, and b is the cooling rate.

The heat dissociated from the exposed surface of the drum $\dot{Q}$ can be estimated by Equation 8.

$$\dot{Q} = -hA_d\left(T_t - T_0\right) \qquad \text{Eq. (8)}$$

where h is a heat transfer coefficient.

Combining Equations 6, 7, and 8, the function of temperature can be generated.

$$T_t = T_0 + e^{-\left(\frac{hA_d}{mc_p}\right)t}\left(T_{t1} - T_0\right) \qquad \text{Eq. (9)}$$

For the repeated braking of a regular time interval, the average temperature T_n at the "nth" brake application is

$$T_{tn} = T_0 + \Delta T\left[\frac{e^{-\left(\frac{hA_d}{mc_p}\right)\Delta t} - e^{-n\left(\frac{hA_d}{mc_p}\right)\Delta t}}{1 - e^{-\left(\frac{hA_d}{mc_p}\right)\Delta t}}\right] \qquad \text{Eq. (10)}$$

After the "nth" application, the temperature T_{n+1} is

$$T_{tn+1} = T_0 + \Delta T\left[\frac{1 - e^{-n\left(\frac{hA_d}{mc_p}\right)\Delta t}}{1 - e^{-\left(\frac{hA_d}{mc_p}\right)\Delta t}}\right] \qquad \text{Eq. (11)}$$

Numerical Example

Compared to the drum brake, a disc brake has little performance losses when high thermal loads occur [20], but also at a higher cost. Therefore, drum brake is still widely used in commercial vehicles.

A long downhill drive and repeated braking are two critical situations for the brake system. Chiaroni and Silveira took the repeated drive cycle as the boundary condition to analyze the drum brake of a passenger vehicle [21]. Palmer and Jansen evaluated the disc brake fidelity by a CFD model [22]. Zeng et al. analyzed the inverse heat conduction of a commercial vehicle drum temperature by the FEM model [23]. Vdovin et al. provided a simulation procedure to numerically predict disc brake system component temperatures of a passenger car during a downhill brake test [24]. According to the national standard GB 12767-2014 in China, during a repeated test, the vehicle needs to decelerate from 60 km/h to 30 km/h in the deceleration of 3 m/s^2, and repeat this process 20 times with 60 s for each time. As the traffic bureau regulated, the maximum speed on the long downhills with different slope angles is shown in Table 1. According to the research of Antanaitis and Lowe [25], the maximum speed on the long downhill in America is about 40 km/h (25 mph).

Take the parameter of a commercial vehicle with a gross mass of 12,000 kg as an example; the relevant parameters are shown in Tables 2 and 3.

To investigate the most critical slope for the long downhill braking, the maximum temperature for different gross vehicle mass (GVM) is calculated and compared in Figure 1. As shown in Table 1 and Figure 1, the energy of the vehicle that runs on a downhill slope is made up of potential energy and kinetic

TABLE 1 Maximum speed on downhills with different slope angles.

Slope (°)	3	4	5	6	7	8	9
Max. speed (km/h)	120	100	80	60	40	30	20

TABLE 2 Parameters of a commercial vehicle.

Gross vehicle weight (kg)	12,000	Drum mass (kg)	39.25
Coefficient of air drag	0.65	Drum expose surface (m^2)	0.127
Projected area (m^2)	6.25	Drum hub volume (m^3)	0.005
Rolling resistance coefficient	0.02		

© Gangfeng Tan

TABLE 3 Thermal parameters of the brake drum.

Temperature (°C)	25	100	200	300
Thermal conductivity ($J \cdot m^{-2} \cdot °C$)	40	40	40.3	38.3
Specific heat ($J \cdot kg/°C$)	480	494	536	557

© Gangfeng Tan

energy. The potential energy is relevant to the slope angle while the kinetic energy is relevant to the speed. The dissipation of the thermal energy is also relevant to the speed. The maximum temperature of the drum increases with the rise of the GVM and increases with the increase of the downhill slope when the slope angle is lower than 6 degrees. When the slope angle is higher than 6 degrees, the maximum temperature decreases due to the lower corresponding kinetic energy. Therefore, for these vehicles, the maximum temperature occurs at the downhill with a slope angle of 6 degrees.

For the repeated braking condition, the maximum temperature of this vehicle can be calculated by Equation 11. The temperature of vehicles with different GVM is shown in Figure 2.

As shown in Figure 2, the temperature rises with the increase of brake time for all the vehicles. The peak value of the temperature rises with the increase of GVM.

FIGURE 1 The maximum temperature of the brake varies with slope and GVM.

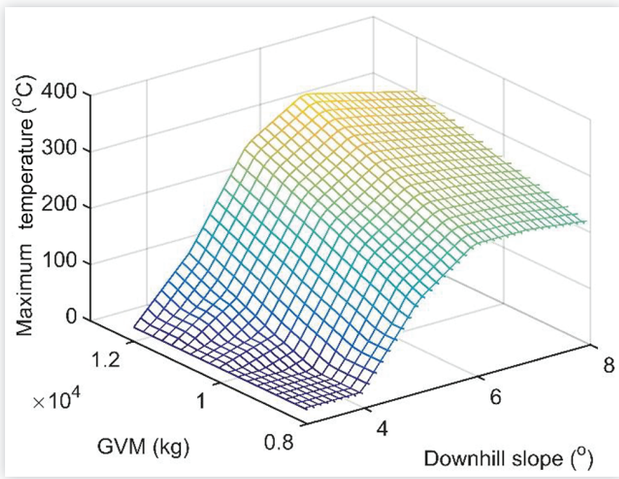

© Gangfeng Tan

FIGURE 2 The brake temperature of vehicles.

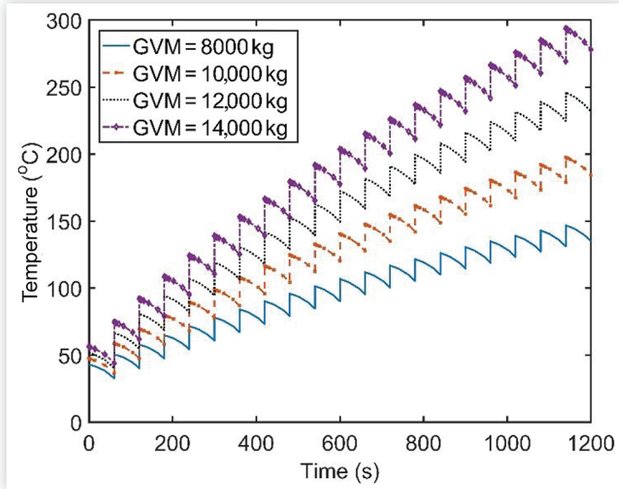

© Gangfeng Tan

According to the temperature in Figures 1 and 2, when the GVM is less than 12000kg, the long downhill test has a more critical requirement on the brake system. Therefore, it is taken as the boundary condition of the forced-air cooling system.

CFD Model Validation and Calibration

Establishment of the CFD Model

As shown in Figure 3, a typical brake drum is complicated and surrounded by a rim and tire. The structure and heat environment of the brake drum is too complicated to analyze using a mathematical model. Therefore, it is simplified, the shoe is ignored, and the bearing and shell are taken as one component; some geometry characteristics such as the filleted corner and small convex plate are ignored. Then a CFD model with 7,456,763 elements is established, as shown in Figure 4.

In this model, the drum is taken as the thermal source, and the tire, rim, and brake drum are established into separated chambers, as shown in Figure 5. The air inlet and outlet surfaces are set in the vehicle driving direction. The air around and inside the drum is built with the fluid element, and the others are built with solid elements. Different materials and properties are assigned to the corresponding parts, as shown in Table 4.

The boundary conditions are described below:

1. The exterior boundary of the air is defined, and the tire, rim, and drum are set into the rotational moving wall.

FIGURE 3 Typical brake drum and simplified wheel system.

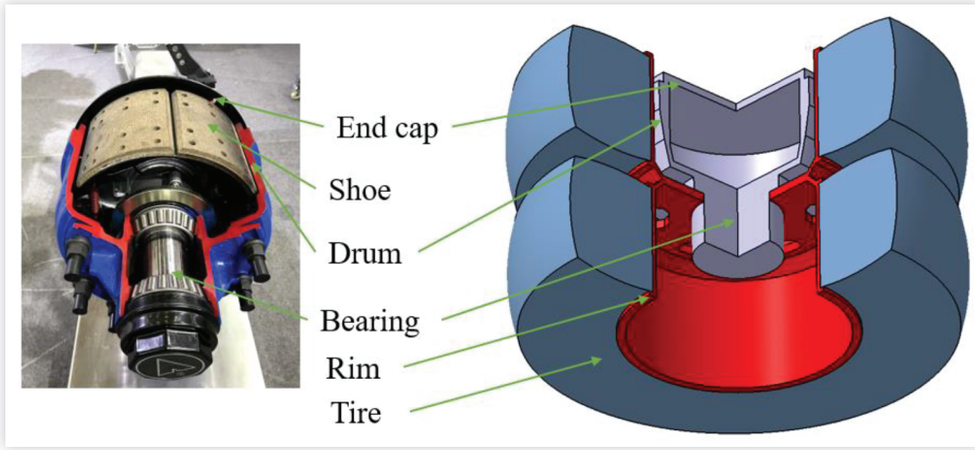

2. The air enters from the inlet surface with the speed of the vehicle velocity, and all flow outlets are maintained at atmospheric pressure.
3. The air in the model is treated as an incompressible ideal gas.

Choose the k-omega model from the viscous models provided by Fluent, and select the SST (Shear Stress Transport) model to initiate the thermal analysis.

Field Test

To improve the accuracy of the CFD model, a field test is initiated on a long downhill. The temperature of the drum and the distance of the vehicle during the journey are recorded by the infrared temperature sensor (as shown in Figure 6) and speed sensor. The detail of the sensors is shown in Table 5. The distance of the vehicle can be gained based on the vehicle velocity from the speed sensor.

It is difficult to find the most crucial downhill road, which has a slope angle of 6 degrees. Therefore, a downhill road with a slope of 5.1 degrees is chosen to finish the field test. The test result, simulation result before and after CFD modification, is shown in Figure 6. It takes about 1400 m to accelerate to the speed of 60 km/h, so for the test result, before 1400 m, the drum temperature is fluctuating around the ambient temperature of 28°C. The field test is terminated as the drum temperature rises to 180°C for safety concerns.

FIGURE 4 CFD model of the brake system.

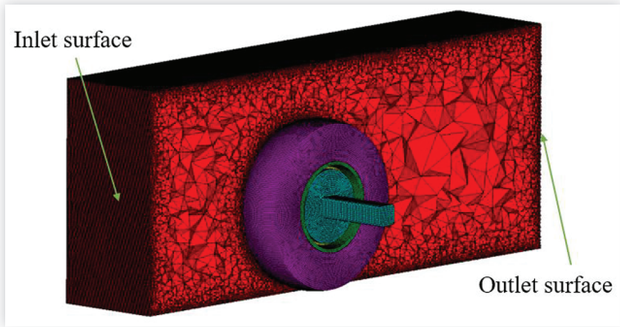

Model Validation and Calibration

Based on the test result, some parameters of the CFD model are modified. Taking the errors into consideration, such as the transmission ratio error and resistance force error, the energy transferred to the drum is adjusted in a proper range, ±10% of the calculated energy. According to this method, a modified model that can acquire a simulation result closer to the result is gained.

According to the comparison in Figure 7, the simulation result of the CFD model has better coherence with the test result than the theoretical model. To compare them more intuitively, the mean absolute percentage error (MAPE) and

FIGURE 5 CFD model of the brake system.

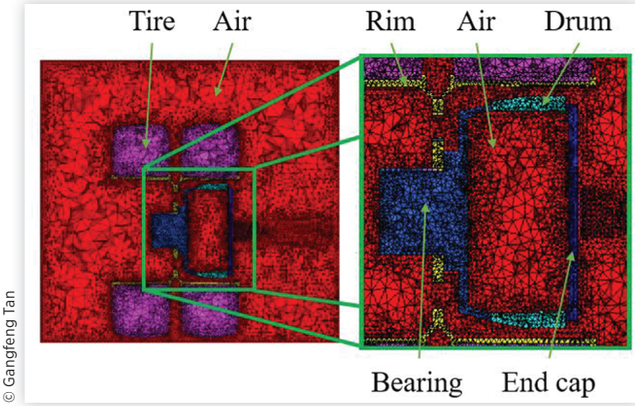

TABLE 4 Property of the CFD model.

Component	Material	Density (kg/m^3)	Thermal conductivity (W/(m·°C))	Specific heat (J/(m·°C))
Air	Air	1.225	0.0242	1006.43
Tire	Rubber	950	0.2	1700
Rim	Aluminum	2719	871	202.4
Bearing/End cap/Drum	Steel	7860	Temperature dependent as described in Table 3	

root mean square error (RMSE) are calculated and compared in Table 6. The result of the modified model has the lowest MAPE and RMSE, which means it has the best coherence relation with the test result.

The gap between the theoretical model and test result may lie in the simplified conditions in the model, such as the heat transfer coefficient h is acquired in the theoretical model as referred from some other similar vehicle.

The simulated temperature is higher than the theoretical value due to the more realistic boundary conditions, including the effect of the rim and tire on the heat dissipation. By modifying the thermal energy transferred to the drum within a proper range, the temperature predicted by the modified model has better coherence with the test result. For the test result, the temperature fluctuates with the slope distance, even with all the necessary measures; there are still some minor errors that cannot be eliminated thoroughly, such as the roughness of the road, the random wind, and unstable speed during the test.

Concept of the Cooling System

Based on the modified CFD model, the maximum temperature of the vehicle in the long downhill with a slope angle of 6 degrees is calculated. As shown in Figure 8, the maximum temperature without the forced-air cooling system can be as high as 291.9°C (the temperature in Figure 8 is shown in kelvin (K), the temperature in Celsius (C) can be gained by adding a constant). For the brake drum in this research, the temperature higher than 200°C will cause a brake regression or failure [26]. It will cause brake regression and damage the safety of the vehicle. According to Figure 9, the velocity streamlines of the airflow around the wheel and brake system stay with the longitudinal direction of the vehicle. In the longitudinal direction, the airflow is sheltered by the wheel hub and tire. It is hard to take away the energy generated by the brake system.

TABLE 5 Detail of the sensors in the field test.

Sensor	Range	Error	Frequency
Infrared temperature sensor	−40 to 600°C	0.1°C	0.2 Hz
Vbox speed sensor	0.5-1600 km/h	0.1 km/h	10 Hz

A forced-air cooling system is designed to lower the temperature rise of the brake, shown in Figure 10. The system is equipped with nozzles near the brake drum that inject airflow in the lateral direction of the vehicle, as the arrows are shown in Figure 10. The airflow comes from the air compressor on the diesel engine to cool the brake down. The nozzles are mounted on the axle and their positions are equally around the drum.

By adding four nozzles in the CFD model and setting the corresponding pressure of the airflow, the temperature of the drum can be gained, as shown in Figure 11. The maximum temperature is decreased to 217.8°C. Compared to the maximum temperature in Figure 8, the temperature is decreased by 74.1°C; the effect of the cooling system is validated.

Based on the experience and basic thermal theory, more airflow or the airflow with a higher speed will lower the temperature in a larger amount. However, they also need more energy to boost. Therefore, it is necessary to optimize the system parameters.

FIGURE 6 Test vehicle and temperature sensor.

FIGURE 7 Comparison of theoretical model and test and simulation results.

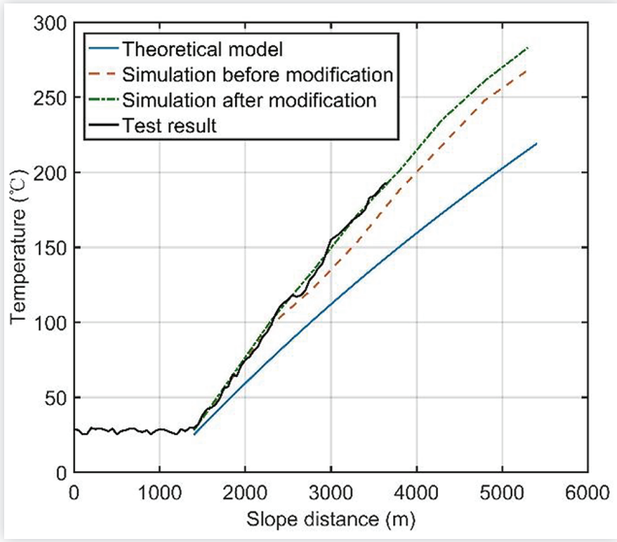

Parameter Optimization

To optimize the parameters of this system, the pressure of the air and the number of nozzles are taken as factors, and the temperature of the drum is taken as the constraint, while the power needed for this system is taken as the objective.

The maximum temperature can be generated by CFD simulation, the nozzle numbers are set to 2, 4, 6, 8 with the air pressure varying from 0.25e5 Pa to 2.5e5 Pa. With these values, 24 CFD models are set and calculated, each model simulation takes about 9 hours.

The power needed can be calculated by the following equations. For the steady flow system, according to the Bernoulli theorem, the energy in this system is conservative like the flow.

$$\frac{v_f^2}{2} - \nabla \tilde{V} + \int \frac{dP}{\rho(P)} = C(\Psi) \qquad \text{Eq. (12)}$$

where v_f is the velocity of the flow, $\nabla \tilde{V}$ is the potential energy of the flow, and $C(\Psi)$ is an integration constant.

If the flow is incompressible and even, Equation 12 can be transformed into Equation 13.

$$\frac{v_f^2}{2} + g\Delta h + \int \frac{dP}{\rho(P)} = C(\Psi) \qquad \text{Eq. (13)}$$

TABLE 6 Validation of the models.

	Theoretical model	CFD before modified	Modified CFD model
MAPE (%)	10.61	3.10	0.98
RMSE (°C)	30.55	10.57	2.99

FIGURE 8 Temperature of the brake drum.

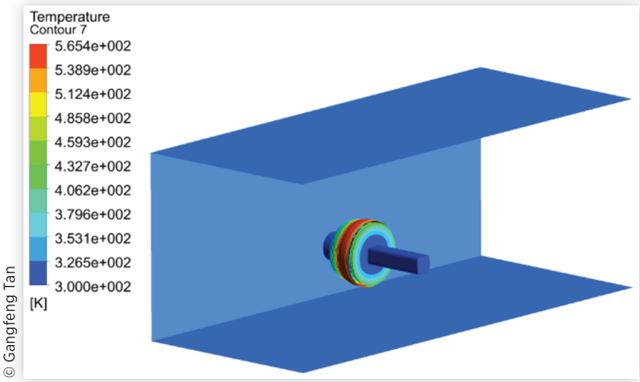

where g is the acceleration of gravity and Δh is the height difference of the inlet and outlet flow. For the inlet flow with the velocity of v_{f1} and outlet flow with the velocity of v_{f2} the pressure difference, ΔP, can be generated by Equation 14.

$$\Delta P = \rho\left(\frac{v_{f1}^2}{2} - \frac{v_{f2}^2}{2} - g\Delta h\right) \qquad \text{Eq. (14)}$$

The power needed to drive the airflow P_p can be expressed as Equation 15.

$$P_p = \Delta P \times \frac{\pi d^2}{4}\left(v_{f2} - v_{f1}\right) \qquad \text{Eq. (15)}$$

In this case, the power needed to drive the nozzles filled with airflow is shown in Figure 12. The power increases as the nozzle number and air pressure increase.

As shown in Figure 13, based on the 24 simulation results, the relationship of the maximum temperature and nozzle number and pressure is established by the RSM, which is widely used in the function setup of factors and objects.

FIGURE 9 Velocity streamlines of the airfloww around the wheel.

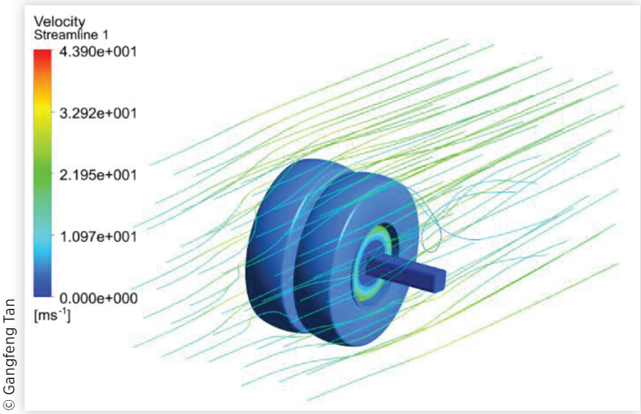

FIGURE 10 Schematic diagram of the forced-air cooling system.

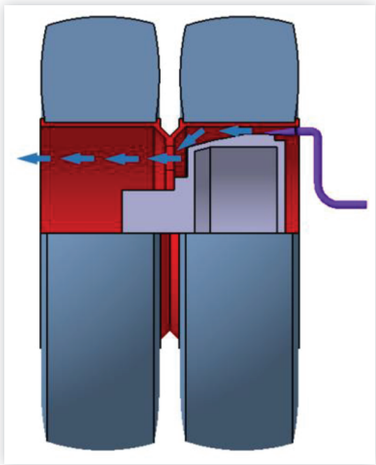

According to the RSM, the maximum temperature of the brake drum, T_{max}, can be generated by Equation 16.

$$T_{max} = 250.11 + 7.36n - 37.52P - 0.13nP - 1.38n^2 + 5.98P^2 \quad \text{Eq. (16)}$$

For the response method, the coefficient of determination, R^2, is used for its validation check. For R^2, the closer the value to 1 the smaller the difference between the predicted value and sample value [27], and this can be generated by Equation 17.

$$R^2 = 1 - \frac{\sum_{i=1}^{n}\left(T_i - \hat{T}_i\right)^2}{\sum_{i=1}^{n}\left(T_i - \bar{T}\right)^2} \quad \text{Eq. (17)}$$

FIGURE 11 Temperature of the brake drum with the air cooling system.

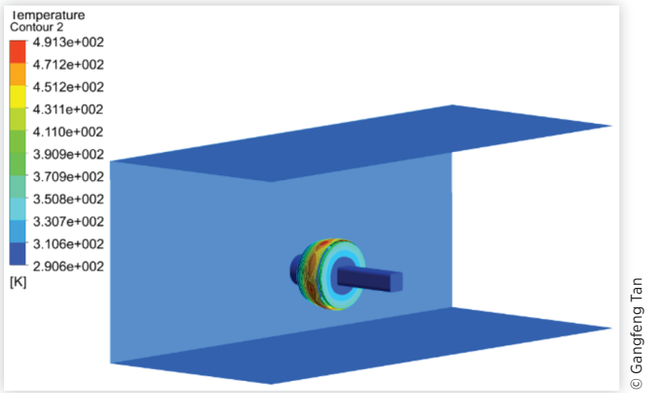

FIGURE 12 The power needed to drive the nozzles filled with airflow.

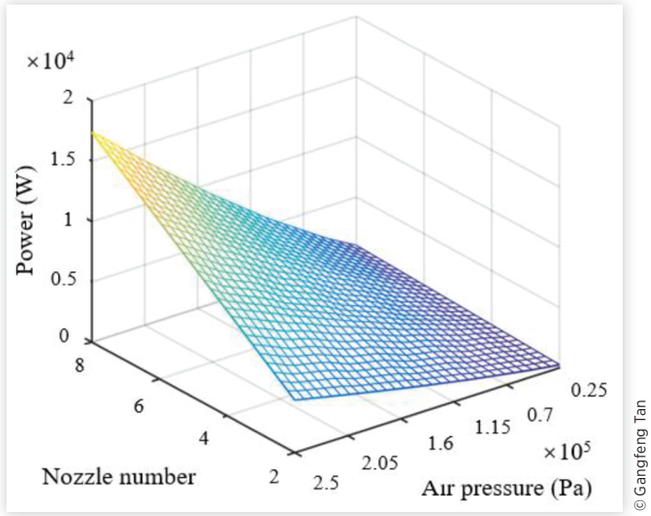

where T_i is the temperature of sample i and $\hat{T}_i$ is the predicted temperature based on sample i. The number of the sample is n and $\bar{T}$ is the mean temperature value of n samples. In this case, the R^2 is 0.96, which means Equation 16 can be used to predict the maximum temperature of the drum in this system. According to Equation 16, the response declines when one factor stays the same while the other one increases.

The adaptive particle swarm optimization (APSO) is based on particle swarm optimization (PSO). PSO is a population-based stochastic approach, which uses the velocity, and a position search model, including a certain number of particles that are used to represent candidates; the position of each particle, x_k, is used to represent a solution of space, and the velocity, v_k, is used to update the

FIGURE 13 Maximum temperature of the brake drum with different nozzles and pressure.

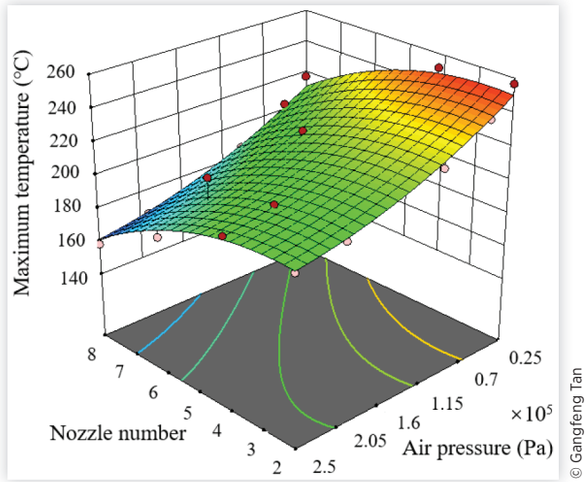

particle position. Each particle searches for better positions in the search space according to its local best position and global best position [28, 29].

$$v_k(i+1)=\omega(i)\times v_k(i)+c_1\times r_1\left(pbest_k(i)-x_k(i)\right)+c_2\times r_2\left(gbest(i)-x_k(i)\right) \quad \text{Eq. (18)}$$

$$x_k(i+1)=v_k(i+1)+x_k(i) \quad \text{Eq. (19)}$$

where k is the particle's index ranging from 1 to N_p, N_p is the population of the particle, i is the iteration number ranging from 1 to i_{max}, r_1 and r_2 are the two numbers that are generated randomly between 0 and 1, c_1 and c_2 are learning factors, *pbest* is the best experience of each particle, and *gbest* is the best experience of all particles in the population. The position and value of the objective function for *pbest* and *gbest* must be stored after each iteration. The iteration begins after the initial evaluation; if the termination criterion is satisfied, the optimal solution reaches *gbest*, and the calculation is ended; otherwise, the iteration repeats. PSO has a quicker convergence, but its limitation is it easily gets stuck in local extremes. To overcome this shortcoming, the nonlinear dynamic weight factor is used to balance the global searching ability and local optimization ability [30]. For the weight factor,

$$\omega(i)=\begin{cases}\omega_{\min}-\dfrac{(\omega_{\max}-\omega_{\min})\times(f(i)-f_{\min})}{f_{avg}-f_{\min}}, & f(i)\le f_{avg}\\ \omega_{\max}, & f(i)>f_{avg}\end{cases} \quad \text{Eq. (20)}$$

where ω_{max} and ω_{min} are the maximum and minimum value of ω, respectively, and $f(i)$ is the current fitness value of the particle, while f_{avg} and f_{min} are the average value and minimum value of all the particles.

When the fitness value of the particles is converging or closing to a local optimum, the weight factor will increase.

FIGURE 14 Fitness value during the optimization.

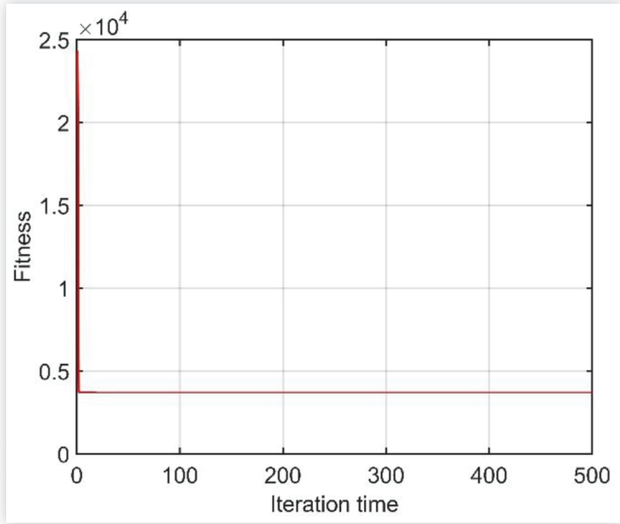

FIGURE 15 Temperature of the drum with the forced-air system.

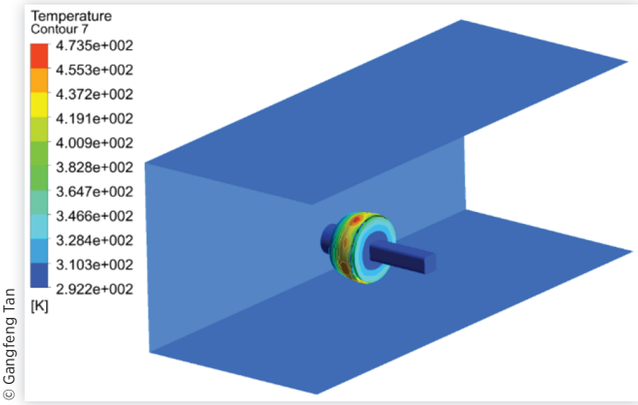

When the fitness value of the particles is dispersing, the weight factor will decrease. If the fitness value is better than the average fitness value, the particle remains due to the low weight factor. Since the weight factor is changing with the fitness value, it is called the adaptive weight factor method.

Based on the APSO and the function of temperature, nozzle number, and air pressure, the optimized parameters can be generated. The fitness value during the optimization is shown in Figure 14.

According to APSO, the best nozzle number and air pressure are gained. Adjust the nozzle number and cross-sectional area based on the optimized nozzle number and the original cross-sectional area. Thus, the nozzle number is rounded off. Take the nozzle number as 6 and pressure as 5.7×10^5 Pa in the simulation model. The drum temperature with the optimized forced-air system is gained, as shown in Figure 15.

With the forced-air cooling system, the maximum temperature of the drum decreases from 291.9°C to 200°C during the most critical work condition (Figure 16). The power needed to generate this system is 3.75 kW, which is within the capability of the air compressor mounted on the engine. When

FIGURE 16 Velocity streamlines in the air around the wheel.

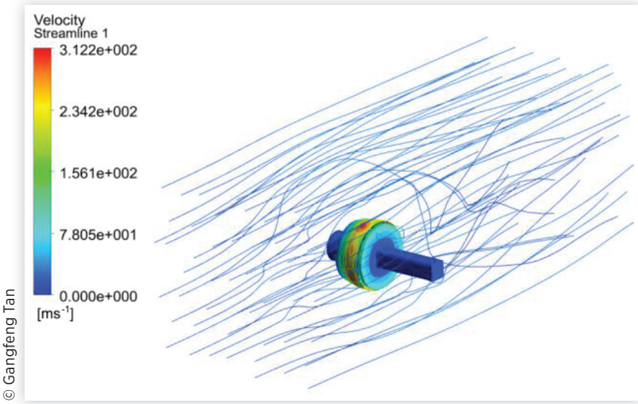

the vehicle is braking, the energy needed to drive the vehicle decreases dramatically, the engine energy is redundant to propel this system.

Conclusion

The safety of the heavy commercial vehicle relies on the brake system. The current water cooling method lowers the vehicle loading capacity by the extra water tank. Based on the analysis of the thermal model of the brake drum, a CFD model of the drum is established and modified by the field test.

Based on the modified CFD model, a new forced-air cooling system is designed and optimized by APSO. For the commercial vehicle with a GVM of 12000 kg, this system can decrease the maximum temperature of the drum from 291.9°C to 200°C, during the most critical long downhill work condition (with a slope angle of 6 degrees and a speed of 60 km/h). The system uses the current air compressor to generate, therefore, no more energy is needed to boost it. Compared to the water cooling method in the current commercial vehicle, the weight of this system is far less than a water tank full of water. Compared to the "duct" solution in the passenger car, it does not damage the air drag or any extra component to turn on or off the "duct."

The parameters of the forced-air cooling system, such as nozzle number, air pressure, and cross-section of the nozzle for vehicles with different GVM, can be adjusted according to the method provided in this article. The most critical work condition relies on the vehicle GVM and work condition; it should be analyzed and determined at the first step. With the proper parameters of this system, the drum temperature can be maintained in a safe range. In the future, a prototype of this system should be made, a field test with the system be initiated to validate the optimization parameters, and some other parameters of this system, such as the transmission loss pressure from the air compressor to the drum, be calibrated.

Acknowledgement

The research is supported by China Ministry of Public Security Application Innovation Project (2018YYCXHBST043) and Suizhou Science and Technology Planning Project (2018SKF-14-31). And the project is funded by Innovative Research Team Development Program of the Ministry of Education of China (IRT_17R83), 111 Project (B17034).

Contact Information

Dr. Gangfeng Tan
Research area: Vehicle dynamic
School of Automobile Engineering Vice-Dean
Associate Professor
Wuhan University of Technology
No. 122 Luoshi Road, Wuhan, Hubei, P.R. China. 430070

References

1. Wang, Q., Qi, G., Zhang, G., and Pu, X., "Study on Brake Durability Dynamometer Experimental Method for Brake NVH and Wear," SAE Technical Paper 2014-01-2520, 2014, https://doi.org/10.4271/2014-01-2520.
2. Yang, Y.C. and Chen, W.L., "A Nonlinear Inverse Problem in Estimating the Heat Flux of the Disc in a Disc Brake System," *Applied Thermal Engineering* 31(14-15):2439-2448, https://doi.org/10.1016/j.applthermaleng.2011.04.008.
3. Singh, O.P., Mohan, S., Venkata Mangaraju, K., Jayamathy, M. et al., "Thermal Seizures in Automotive Drum Brakes," *Engineering Failure Analysis* 17(5):1155-1172, https://doi.org/10.1016/j.engfailanal.2010.02.001.
4. Mule, N., Pilane, D., Mahale, P., and Raajha, M., "FEA Analysis and Correlation of Thermo-Mechanical Deformations of a Disc Brake Rotor," SAE Technical Paper 2015-26-0206, 2015, https://doi.org/10.4271/2015-26-0206.
5. Hwang, P. and Xuan, W., "Investigation of Temperature and Thermal Stress in Ventilated Disc Brake Based on 3D Thermo-Mechanical Coupling Model," *Journal of Mechanical Science and Technology* 24(1):81-84, https://doi.org/10.1007/s12206-009-1116-7.
6. Martinez Laurent, J., Jordan, A., and Canales, F., "CFD-CAE Multi-Physics Simulation Approach for Brake Disc Thermal Coning," SAE Technical Paper 2014-01-2493, 2014, https://doi.org/10.4271/2014-01-2493.
7. Bhambare, K., Haffey, M., and Jelic, S., "Brake Duty Cycle Simulation for Thermal Design of Vehicle Braking System," SAE Technical Paper 2013-36-0015, 2013, https://doi.org/10.4271/2013-36-0015.
8. Travaglia, C.A.P., Araujo, J., Bochi, M., Yoneda, A. et al., "Analysis of Drum Brake System with Computational Methods," SAE Technical Paper 2013-36-0022, 2013, https://doi.org/10.4271/2013-36-0022.
9. Anil Shah, A. and Patidar, A., "Conversion of Drum Brake System to Disc Brake with CAE and CFD: Resulted in Optimized Brake Rotor Design and Improved Performance," SAE Technical Paper 2017-26-0261, 2017, https://doi.org/10.4271/2017-26-0261.
10. Mahammad, I., Nagaraj, V., and Prabhakar, S., "CFD and CAE Approach for Brake Rotor Thermal Analysis," SAE Technical Paper 2017-26-0292, 2017, https://doi.org/10.4271/2017-26-0292.
11. Raja, T., Mathiselvan, G., Sreenivasulureddy, M., and Goldwin Xavier, X., "Design and Analysis of Air Flow Duct for Improving the Thermal Performance of Disc Brake Rotor," Paper Presented at in *IOP Conference Series: Materials Science and Engineering*, Chennai, India, Jan. 1-3, 2017.
12. Ocampo, J., Jelic, S., and Han, J., "Simulation-Driven Process to Evaluate Vehicle Integration Aspects in Brake Thermal Design," SAE Technical Paper 2017-36-0011, 2017, https://doi.org/10.4271/2017-36-0011.
13. Kim, G., Park, J., Lee, B., and Hwang, H., "A Study on Optimization of Brake Cooling System Considering

Aerodynamics," SAE Technical Paper 2018-01-1875, 2018, https://doi.org/10.4271/2018-01-1875.

14. Sunday, B., Aminu, U., Yahaya, P.O., and Ndaliman, M.B., "Development and Analysis of Finned Brake Drum Model Using Solidworks Simulation," *International Journal of Innovative Research in Science, Engineering and Technology* 4(5):3651-3658, 2015, https://doi.org/10.15680/IJIRSET.2015.0405115.
15. Wei, D., Alian, C., Bo, S., and Chenghui, Z., "Multi-Objective Optimal Operation and Energy Coupling Analysis of Combined Cooling and Heating System," *Energy* 98:296-307, 2016, https://doi.org/10.1016/j.energy.2016.01.027.
16. Soheyli, S., Mohamad, H., and Mehri, M., "Modeling a Novel CCHP System Including Solar and Wind Renewable Energy Resources and Sizing by a CC-MOPSO Algorithm," *Applied Energy* 184:375-395, 2016, https://doi.org/10.1016/j.apenergy.2016.09.110.
17. Li, C., Jie, J., and Liangkun, Y., "A Comparative Experimental Study on Thermal Fade Performance of Disc and Drum Brakes," *Qiche Gongcheng/Automotive Engineering* 39(12):1397-1401 and 1430, 2017, https://doi.org/10.19562/j.chinasae.qcgc.2017.12.007.
18. Holmberg, K., Peter, A., Nils-Olof, N., Kari, M. et al., "Global Energy Consumption due to Friction in Trucks and Buses," *Tribology International* 78:94-114, 2014, https://doi.org/10.1016/j.triboint.2014.05.004.
19. Newcomb, T.B. and Spurr, R.T., "Commercial Vehicle Braking System Definitions," (No. Monograph, 2002), 103-105, https://doi.org/10.4271/J2627_200209.
20. Gohring, E. and Von Glasner, E.C., "Performance Comparison of Drum and Disc Brakes for Heavy Duty Commercial Vehicles," SAE Technical Paper 902206, 1990, https://doi.org/10.4271/902206.
21. Chiaroni, A.B. and Silveira, Z.C., "Thermal Analysis of a Rear Drum Brake for Lightweight Passenger Vehicles," SAE Technical Paper 2014-36-0112, 2014, https://doi.org/10.4271/2014-36-0112.
22. Palmer, E. and Jansen, W., "Development of a High Fidelity CAE Model for Predicting Brake System Temperatures," SAE Technical Paper 2017-01-0145, 2017, https://doi.org/10.4271/2017-01-0145.
23. Zeng, S., Zhang, H., and Meng, Y., "Research on Heat Conduction Inverse Problem of Continuous Long Downhill Truck Brake," Paper Presented at in *2016 International Conference on Civil, Transportation and Environment*, Guangzhou, China, Jan. 30-31, 2016.
24. Vdovin, A., Mats, G., and Simone, S., "A Coupled Approach for Vehicle Brake Cooling Performance Simulations," *International Journal of Thermal Sciences* 132:257-266, 2018, https://doi.org/10.1016/j.ijthermalsci.2018.05.016.
25. Antanaitis, D.B. and Lowe, B., "Braking with a Trailer and Mountain Pass Descent," SAE Technical Paper 2019-01-2116, 2019, https://doi.org/10.4271/2019-01-2116.
26. Xu, Y., Mei, B., Xiao, L., Xia, W. et al., "Combined Hill Descent Braking Strategy for Heavy Truck in the Featured-Slope," SAE Technical Paper 2017-01-2535, 2017, https://doi.org/10.4271/2017-01-2535.
27. Montgomery, D.C., *Design and Analysis of Experiments* Fourth Edition (New York: Wiley, 1997).
28. Eberhart, R. and Kennedy, J., "A New Optimizer Using Particle Swarm Theory," in *MHS'95. Proceedings of the Sixth International Symposium on Micro Machine and Human Science*, Nagoya, Japan, 1995, 39-43.
29. Shi, Y. and Eberhart, R., "A Modified Particle Swarm Optimizer," in *1998 IEEE International Conference on Evolutionary Computation Proceedings. IEEE World Congress on Computational Intelligence* (Cat. No. 98TH8360), Anchorage, AK, 1998, 69-73.
30. Lanlan, K., "Several Improvements to Particle Swarm Optimization and Their Theoretical Fundamentals," Ph.D. dissertation, Wuhan University, 2017.